OPTOELECTRONICS AND ADVANCED MATERIALS – RAPID COMMUNICATIONS Vol. 4, No. 8, August 2010, p. 1166 - 1169

# Multifunctional $TiO_2$ nanowires-modified nanoparticles bilayer film for 3D dye-sensitized solar cells

H. WANG [a,b], Y. LIU[A], M. LI [a,b], H. HUANG [c], Hong-mei XU [a], Rui-jiang HONG[*a], H. SHEN[a]
[a] *School of Physics and Engineering, Institute for Solar Energy Systems , State Key Laboratory of Optoelectronic Materials and Technologies, Sun Yat-sen University, Guangzhou 510275, China*
[b]*Faculty of Material Science & Engineering, Guilin University of Technology, Guilin 541004, China*
[c]*Instrument analysis and research center, Sun Yat-sen University, Guangzhou 510275, China*

The radial free-standing $TiO_2$ nanowires were rooted into $TiO_2$ nanoparticles film coated Ti wire via a facile hydrothermal method. This $TiO_2$ nanowires-modified nanoparticles bilayer film acted as a multifunctional role for enhancing solar cells efficiency: light trapping, modification of thin film surface cracks, electricity-generation properties and providing fast electron transfer pathway. The study results revealed that the three-dimensional (3D) dye-sensitized solar cells fabricated with $TiO_2$ bilayer film increased by 32.7% in the max output power as compared to the $TiO_2$ NPs film under AM1.5G condition. This increase is mainly attributed to the better light scattering of the $TiO_2$ bilayer film.

(Received June 27, 2010; accepted August 12, 2010)

*Keyords*: Nanowire, Nanoparticle, $TiO_2$, Solar cell

## 1. Introduction

There has been an active research for dye-sensitized solar cells (DSSCs) due to their low cost and high energy conversion efficiency combined with a facile fabrication process [1-3]. The photoanode of conventional DSSCs commonly consists of a nanocrystalline $TiO_2$ nanoparticles (NPs) layer film, which provides a large surface for absorption of light-harvesting molecules [4]. However, multiple trapping/detrapping events occurring within grain boundaries result in a slow electron transport rate in the NPs film [5-8]. Furthermore, current densities only achieve 55 ~ 75% of their theoretical maxima at full sunlight by using the dyes with the poor absorption of red and near-infrared light, and the thickness of the porous thin film can't be increased at will without affecting its mechanical properties.[9] One promising solution is employing light scattering structures such as some metal oxide particles layer with several hundreds nanometer diameter or admixture of some larger particles to increase the average optical path length of the light within the film [10-13]. However, these scattering NPs hardly provide a large specific surface area for dye molecular adsorption. One-dimensional (1D) oriented nanowires(NWs) have attracted much attention for its application in DSSCs, due to its fast electron transport pathway and high specific surface area [14]. However, most of 1D $TiO_2$ NWs have been limited to application in a back-side illuminated DSSCs due to the in situ growth of 1 D NWs on the opaque titanium substrate unless the transfer of $TiO_2$ NWs from titanium substrate to TCO glass [15-17].

A unique , 3D DSSC based on all titanium wire substrate has been reported by our group [18-20]. This cell exhibits superiority of absorbing sunlight from all directions. To further improve the efficiency of the 3D DSSC, here we present the bilayer film of $TiO_2$ NWs-modified $TiO_2$ NPs by a simple hydrothermal method instead of the mixing method.

## 2. Experimental

### 2.1. Reagents

All chemical reagents were commercial available, including LiI (anhydrous, ≥98%), $I_2$ (≥99.55(RT)), titanium (IV) isopropoxide (≥98%) of Fluka, 4-tertbutylpyridine (99%) of Aldrich. Cis-bis(isothiocyanato)bis(2,2'-bipyridyl-4,4'-dicarboxylato)-ruthenium(II) bis-tetrabutylammonium (N719, Solaronix). $TiO_2$ powder (P25) was supplied by Degussa. Designation of industrial pure Ti wires were TA1. Chloroplatinic acid ($H_2PtCl_6 \cdot 6H_2O$) came from Shenyang Institute of Nonferrous Metals, China.

### 2.2. Measurement

The morphology and dimensions of the as-synthesized various $TiO_2$-based nanomaterials were observed by field-emission scanning electron microscopy (FESEM, LEO 1550 VP) equipped with EDS. The crystal structure of the as-prepared film was analyzed using XRD (SHIMADZU XRD-6000) with Cu Kα radiation. Current-voltage (I-V) characteristics of the cells under simulated sunlight (Oriel xenon lamp, AM 1.5 was determined by a standard silicon solar cell) were recorded using a digital sourcemeter (Keithley,

2400). Reflectivity and transmittance spectra of samples were analyzed by a UV-Visible-NIR spectrophotometer (HITACHI, U-4100).

### 2.3. Preparation of photoanodes based on $TiO_2$ NPs

The method for the preparation of $TiO_2$ colloid followed the procedure described as follows [11]. 12 g $TiO_2$ powder was ground in a porcelain mortar with 4 mL ethanol containing 0.4 mL acetylacetone for about 30 min and it was diluted by slow addition of water under continued grinding. Finally, a detergent (0.2 mL Triton X-100) was added. The spiral electrode, with 0.19 cm outer diameter and 1 cm in length, was made from 0.3 mm diameter and 7.5 cm in length titanium wire was washed in ultrasonic bath, and then coated with $TiO_2$ film by sol-gel dip-coating process followed by heat treatment at 450 ℃ for 30 min.

### 2.4. $TiO_2$ NWs synthesis

The as-prepared photoanodes were placed in a Teflon-lined vessel containing 26 mL of 1.0 mol/L NaOH solution. Afterward, the vessel was sealed and then hydrothermally heated at 230 ℃ for 4 h. Thus-treated samples were immersed in 0.1 mol/L HCl for 10 h, and then rinsed with deionized water. Finally, they were heated at 450 ℃ for 30 min. All photoanodes coated with NPs film and NWs/NPs bilayer film were immersed in a $5\times10^{-4}$ mol/L solution of N719 in dry ethanol and refluxed at 80 ℃ for 3 h to fix dye on $TiO_2$ film.

### 2.5. Preparation of the counter electrode

The Ti wires, 0.6 mm in diameter, were used as counter electrode substrate. The textured surface was produced by exposing the substrate to an etching fluid comprising a hydrofluoric acid and a nitric acid. Then the Ti wires were washed with acetone and ethanol in an ultrasonic bath for 3 min.

The Pt film was coated on Ti wires by the electrodeposition process. Electrodeposition was carried out using an aqueous solution of $5\times10^{-3}$ mol/L $H_2PtCl_6\cdot6H_2O$ at room temperature. A digital sourcemeter (Keithley, 2400) was applied as a power supply. Here, Pt electrode was prepared with 15 mA $cm^{-2}$ current density for 5 s and then calcined at 150 ℃ for 30 min.

### 2.6. $TiO_2$ NWs/$TiO_2$ NPs based DSSC assembly

The schematic structure and principles of 3D DSSC with a bilayer film are shown in Fig. 1. The platinum electrode was put into the inner hole of the spiral photoelectrode, and then they were put into the glass tube. The electrolyte, consisting of 0.5 mol/L LiI, 0.05 mol/L $I_2$, and 0.5 mol/L 4-tert-butylpyridine in acetonitrile, was also introduced to the tube. Finally, it was sealed with stuffing and epoxy.

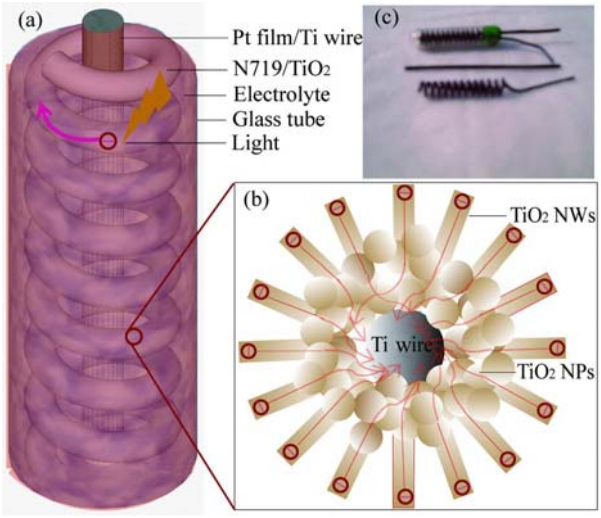


*Fig. 1. (a) Schematic diagram of the 3 D DSSC. (b) Radially oriented $TiO_2$ NWs modified-$TiO_2$ NPs was coated onto spiral Ti wire, and the arrows indicate the path of the electron transfer within the bilayer film. (c) A picture of the 3D DSSC.*

## 3. Results and discussion

Fig. 2 shows scanning electron microscopy (SEM) images of a $TiO_2$ NWs/$TiO_2$ NPs bilayer film coated onto the spiral Ti wire substrate (Fig. 2(a)). Radial oriented $TiO_2$ NWs are uniformly self-assembled onto the $TiO_2$ NPs, and rooted firmly inside the $TiO_2$ NPs. The thickness of the NWs film and the NPs was as much as ~2 μm. Interestingly, the partial $TiO_2$ NPs films layer was replaced by the $TiO_2$ NWs film layer shown in Fig. 2a inset, which was different from the $TiO_2$ NWs and $TiO_2$ NPs mixture structure reported in the previous literature.[8-10] The $TiO_2$ NWs arrays were 20 ± 5 nm in diameter (Fig. 2(b)). Commercially obtained P25 $TiO_2$ NPs had diameters of 23-25 nm, as depicted in Fig. 2(c). The corresponding X-ray diffraction (XRD) patterns recorded from the $TiO_2$ NPs and $TiO_2$ NWs/$TiO_2$ NPs are shown in Fig. 2d, respectively. It is clear from the results that the $TiO_2$

NPs was partially converted into $TiO_2$ NWs without other phase transformation.

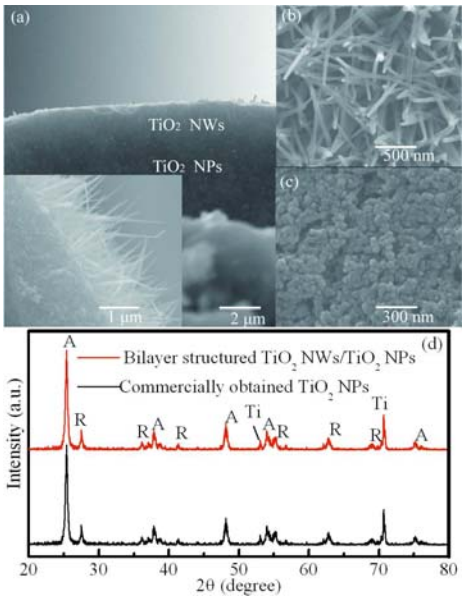


*Fig. 2. SEM image of a bilayer structure showing (a) cross-sectional of $TiO_2$ NPs underlayer and $TiO_2$ NWs overlayer; the inset shows a high magnification SEM image of the as-synthesized bilayer film, (b), (c) high-magnified observation of each layer, and (d) XRD patterns from the sintered $TiO_2$ NPs and bilayer film.*

For a comparison, we fabricated the $TiO_2$ NWs/$TiO_2$ NPs bilayer based DSSC and P25 $TiO_2$ NPs based DSSC, respectively. J-V characteristics of the two DSSCs were obtained under AM 1.5G illumination (100 mW/cm$^2$). Fig. 3 shows the J-V curve of the two cells. It can be seen that the $TiO_2$ NWs/$TiO_2$ NPs bilayer based cell indicated higher short-circuit current density and the max power output than the $TiO_2$ NPs based cell. The max power output was enhanced by 32.7%.

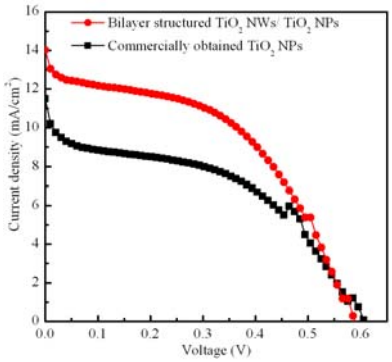


*Fig. 3. The J-V curves of 3D DSSC consisting of $TiO_2$ NWs/ $TiO_2$ NPs bilayer film, comparing with that of $TiO_2$ NPs film under AM1.5G illumination.*

The diffuse reflectance spectra of $TiO_2$ NPs layer and $TiO_2$ NWs/$TiO_2$ NPs bilayer were measured by spectrophotometer. As shown in Fig. 4a, the reflectance spectra of $TiO_2$ NPs layer coated onto titanium sheet was measured firstly, after hydrothermal reaction, the formed $TiO_2$ NWs/$TiO_2$ NPs bilayer was then measured. It can be seen that the $TiO_2$ NWs/$TiO_2$ NPs bilayer film exhibited a substantially lower diffuse reflectance than the $TiO_2$ NPs film in the spectral range from 400 to 800 nm. The average reflectance of sample made from $TiO_2$ NPs only was about 42.5% and is decreased to about 29.6% for $TiO_2$ NWs/ $TiO_2$ NPs film. The incident light could be reflected much more times by $TiO_2$ NWs between the $TiO_2$ NWs and $TiO_2$ NPs bilayer film, which would enhance the light absorption ability of $TiO_2$ NWs/ $TiO_2$ NPs bilayer film. Therefore, the increased higher current and power output for the $TiO_2$ NWs/ $TiO_2$ NPs compared to the $TiO_2$ NPs may be a consequence of better light trapping.

Fig. 4b shows that the reflectance of the $TiO_2$ NPs layer and $TiO_2$ NWs/$TiO_2$ NPs bilayer after dye adsorption on the film decreases drastically at the spectral range 400-800 nm, which is mainly due to light adsorption by the dye molecules. The dye-sensitized $TiO_2$ NWs/$TiO_2$ NPs bilaye film exhibits the reflectance of 12.1%, which was lower than that (15.7%) of $TiO_2$ NPs layer film at the spectral range 400-800 nm. indicating a better light trapping within the bilayer film. Therefore, the max power output in Fig. 3 for the bilayer film compared to the $TiO_2$ NPs film is a consequence of better light trapping.

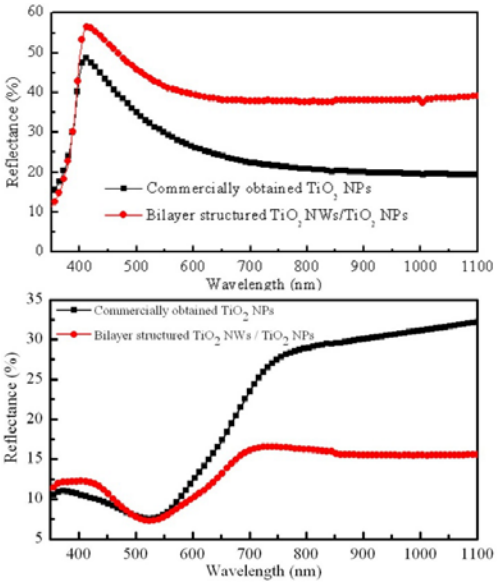


*Fig. 4. Diffused reflectance spectra of the $TiO_2$ NPs and $TiO_2$ NWs/$TiO_2$ NPs bilayer film (a) without and (b) with adsorbed N719 dye.*

Further studies showed that $TiO_2$ NWs were helpful to modify surface cracks of $TiO_2$ NPs film. The crack-free surface morphology of bilayer film compared to the $TiO_2$ NPs film was observed (Fig. 5a-c). The existing cracks in the $TiO_2$ NPs film (Fig. 5a) may act as electron traps that hamper the movement of electrons,

and increase the charge recombination of triiodide and metal substrate. As shown in Fig. 5b and 5c, not only the cracks were connected with $TiO_2$ NWs like bridge, but also the $TiO_2$ NWs were rooted into the $TiO_2$ NPs layer (Fig. 2a inset), indicating a close connectivity between $TiO_2$ NWs and $TiO_2$ NPs, which helped to preserve the crack-free thin films. This occurrence may mainly be the direct contact between the NaOH aqueous solution and surface of $TiO_2$ NPs film. NaOH aqueous solution may penetrate into the surface cracks of $TiO_2$ NPs film, thus leading to the growth of $TiO_2$ NWs within the cracks according to the reaction mechanism [14]. The bilayer film formation process is shown in Fig. 5d and 5e. The interface of the proposed bilayer film may have an excellent crystal lattice match between the $TiO_2$ NWs and $TiO_2$ NPs, due to in-situ growth of $TiO_2$ NWs on the $TiO_2$ NPs, which is different from other fabrication combination process, such as layer-by-layer [15-18] atomic layer deposition, [19-21] and sol-gel process [22]. Generally, more cracks and pores tend to appear when the film becomes thicker. Therefore, applying $TiO_2$ NWs to the further surface treatment of $TiO_2$ NPs film is very significant, especially for its application in the DSSCs. More importantly, these findings have suggested a general method to eliminate surface cracks of $TiO_2$ NPs film. In addition, for the bilayer film DSSC, the thickness of the underlayer $TiO_2$ NPs film can be further tuned by overlayer $TiO_2$ NWs through varying the different hydrothermal conditions, such as the reaction time, temperature, and the NaOH concentration. A higher solar cell efficiency will be expected to be obtained using this process.

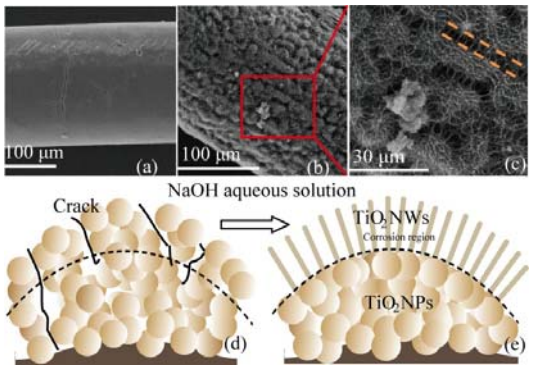


*Fig. 5. Surface SEM images of the $TiO_2$ thin film. (a) Before hydrothermal reaction; (b) After hydrothermal reaction; (c) A high magnification image of bilayer film. The scheme for surface morphology of $TiO_2$ NPs film before hydrothermal growth (d), and (e) after hydrothermal growth.*

## 4. Conclusions

In conclusion, $TiO_2$ NWs/$TiO_2$ NPs bilayer film was realized by sol-gel dip-coating process in combination with a facial hydrothermal method. Compared with a $TiO_2$ NPs DSSC, the DSSC with a $TiO_2$ NWs/$TiO_2$ NPs bilayer film achieved a higher max output power. The relatively high efficiency is attributed to light trapping, a crack-free surface, and fast electron transfer pathway provided by $TiO_2$ NWs/$TiO_2$ NPs bilayer film. Furthermore, by adjusting the thickness of each layer of the bilayer film, the 3D DSSC is expected to obtain higher conversion efficiency. Apart from application in the proposed 3D DSSC, the $TiO_2$ NWs/$TiO_2$ NPs bilayer film may be used in the conventional DSSCs and other applications, such as chemical and biological sensors, and so on.

**Acknowledgments**

This work is supported by the National Natural Science Foundation of China (Grant No. 50702079), and the National High-Tech Research and Development Program of China (Grant No. 2006AA05Z409).

## References

[1] B. Oregan, M. Grätzel, Nature (London), **353**, 737-740 (1991)..
[2] A. Hagfeldt, M. Grätzel, Acc. Chem. Res, **33**, 269-277 (2000).
[3] A. Kay, M. Grätzel, Sol. Energy Mater. Sol. Cells, 1996, **44**, 99-117.
[4] N. Kopidakis, E. A. Schiff, N. G. Park, J. van de Lagemaat, A. J. Frank, J. Phys. Chem. B, **104**, 3930-3936 (2000).
[5] J. Nelson, Phys. Rev. B, **59**, 15374 (1999).
[6] L. Forro, O. Chauvet, D. Emin, L. Zuppiroli, H. Berger, F. Levy, J. Appl. Phys, **75**, 633-635 (1994).
[7] Sanehira, Yoshitaka, Uchida and Satosh, Kagaku Kogyo, **55**, 796-800 (2004).
[8] Y. Suzuki, S. Ngamsinlapasathian, R. Yoshida, S. Yoshikawa, Cent. Eur. J. Chem, **4**, 476-488 (2006).
[9] B. Tan, Y. Y. Wu, J. Phys. Chem. B, **110**, 15932-15938 (2006).
[10] K. Asagoe, S. Ngamsinlapasathian, Y. Suzuki, S. Yoshikawa, Cent. Eur. J. Chem, **5**, 605-619 (2007).
[11] Y. Liu, H. Shen, Y. Deng, Sci Chin Ser E, **49**, 663-673 (2006).
[12] H. Wang, Y. Liu, M. Li, H. Huang, M. Y. Zhong, H. Shen, Appl. Phys. A: Mater. Sci. Process, **97**, 25-29 (2009).
[13] Y. Yoshida, S. S. Pandey, K. Uzaki, S. Hayase, M. Kono, Y. Yamaguchi, Appl. Phys. Lett., **94**, (2009).
[14] D. Li, Y. L. Wang, Y. N. Xia, Nano Lett, **3**, 1167-1171 (2003).
[15] A. O. T. Patrocinio, L. G. Paterno, N. Y. M. Iha, J. Photochem. Photobiol A-Chem, **205**, 23-27 (2009).
[16] G. M. Lowman, P. T. Hammond, Small, **1**, 1070-1073 (2005).
[17] H. Tokuhisa, P. T. Hammond, Adv. Funct. Mater., **13**, 831 (2003).
[18] J. A. He, R. Mosurkal, L. A. Samuelson, L. Li, J. Kumar, Langmuir, **19**, 2169-2174 (2003).
[19] M. Law, L. E. Greene, A. Radenovic, T. Kuykendall, J. Liphardt, P. D. Yang, J. Phys. Chem. B, **110**, 22652-22663 (2006).
[20] L. E. Greene, M. Law, B. D. Yuhas, P. D. Yang, J. Phys. Chem. C, **111**, 18451-18456 (2007).
[21] T. C. Li, M. S. Goes, F. Fabregat-Santiago, J. Bisquert, P. R. Bueno, C. Prasittichai, J. T. Hupp, T. J. Marks, J. Phys. Chem. C, **113**, 18385-18390 (2009).
[22] Y. M. Lee, C. H. Lai, Solid-State Electronics, **53**,

1116-1125 (2009).

*Corresponding author: hongruij@mail.sysu.edu.cn